

# Direct temporal measurement of hot-electron relaxation in a phonon-cooled metal island

D. R. Schmidt, C. S. Yung, and A. N. Cleland\*

Department of Physics and iQUEST, University of California at Santa Barbara, Santa Barbara, CA 93106

(Dated: November 21, 2018)

We report temporal measurements of the electronic temperature and the electron-phonon thermal relaxation rate in a micron-scale metal island, with a heat capacity of order 1 fJ/K ( $C \sim 10^7 k_B$ ). We employed a superconductor-insulator-normal metal tunnel junction, embedded in a radio-frequency resonator, as a fast ( $\sim 20$  MHz) thermometer. A resistive heater coupled to the island allowed us to drive the electronic temperature well above the phonon temperature. Using this device, we have directly measured the thermal relaxation of the hot electron population, with a measured rate consistent with the theory for dynamic electron-phonon cooling.

PACS numbers: 65.90.+i, 63.20.Kr, 65.40.Ba

Measurement of the heat capacity  $C$  of a thermodynamic system, in contact with a thermal reservoir through a thermal conductance  $G$ , necessitates the measurement of temperature over time scales shorter than the characteristic thermal relaxation time  $\tau = C/G$ . For mesoscopic devices, this time scale becomes exceedingly short, as both the electron and phonon heat capacities scale with device volume  $V$ . Furthermore, it is difficult to thermally isolate a phonon system from its environment, as even a very weak mechanical suspension is limited at low temperatures by the scale-independent quantum of phonon thermal conductance [1, 2, 3, 4]. Electrons in a metal however naturally decouple from their phonon environment at low temperatures, with an electron-phonon thermal conductance  $G_{e-p} \propto VT^4$ . As the electron heat capacity scales as  $C_e \propto VT$ , the electron-phonon thermal relaxation time  $\tau_{e-p} = C_e/G_{e-p}$  is independent of volume, and scales as  $T^{-3}$ . At 1 K,  $\tau_{e-p}$  is of order 10 nanoseconds, a time scale that is accessible using a radio-frequency superconductor-insulator-normal metal (rf-SIN) tunnel junction thermometer [5].

In this letter, we present large-bandwidth measurements of the electronic temperature of a micron-scale metal island. Our measurement has ample bandwidth with which to directly measure  $\tau_{e-p}$  at temperatures up to 1 K. This system therefore allows us to probe the thermodynamic behavior of electrons in very small metal volumes, potentially with heat capacities as small as  $10 k_B$ . Such small metal volumes are prime candidates for energy absorbers in far-infrared photon-counting bolometers [3], and would allow unprecedented calorimetric sensitivity in the mesoscopic regime. Measurements over time scales shorter than  $\tau_{e-p}$  are also critical for developing a complete understanding of the thermodynamics of mesoscopic systems.

The thermal decoupling of electrons and phonons at low temperatures was first described theoretically by Little [6], with a more general discussion provided by Gantmakher [7]. For a bulk metal with volume  $V$ , the power flow  $P_{e-p}$  from the electron gas at temperature  $T_e$  to the phonon gas at  $T_p$  is given by

$$P_{e-p} = \Sigma V (T_e^n - T_p^n), \quad (1)$$

where  $\Sigma$  is a material-dependent parameter. For a spherical

Fermi surface and a Debye phonon gas,  $n = 5$ .

A number of researchers have verified that Eq. (1) applies to the static heating of thin-film metals, albeit with  $n$  slightly lower than 5 (fit values for  $n$  fall in the range from 4.5 to 4.9, with values for  $\Sigma$  in the range  $1 - 2 \times 10^9$  W/m<sup>3</sup>-K<sup>5</sup> [8, 9]). These measurements were made using a dc superconducting quantum interference device (dc-SQUID) to measure the Johnson-Nyquist noise in the metal film, and thus extract the electronic temperature.

A second approach to measuring the electron temperature in thin metal films was presented by Nahum *et al.* [10]: using a SIN tunnel junction as an electronic thermometer. These authors suggested that such a structure could form the heart of a bolometric detector. Measurements of the static energy distribution of electrons in a normal metal under voltage bias were made by Pothier *et al.* using a similar SIN-based thermometer [11]. Yung *et al.* [3] also demonstrated a SIN thermometer in contact with a normal metal island, the whole fabricated on a micron-scale suspended GaAs substrate.

Here we study the *dynamic* temperature response of a small metal island using a SIN tunnel junction thermometer. Well below the superconducting transition temperature  $T_C$ , the tunnel junction's small-signal resistance at zero bias,  $R_0 \equiv dV/dI(0)$ , is exponentially dependent on the ratio of temperature  $T$  to the superconducting energy gap  $\Delta$ ,  $R_0 \propto e^{\Delta/k_B T}$ . A sub-micron scale SIN tunnel junction therefore has a low-temperature resistance that can easily exceed  $10^6 \Omega$ , limiting conventional time-domain measurements to bandwidths of order 1 kHz. In order to monitor changes in this resistance at sub-microsecond time scales, we circumvent the unavoidable stray capacitance in the measurement circuit by embedding the junction in a  $LC$  resonant circuit, as shown in Fig. 1 [12]. We then measure the resistance of the SIN junction, and thus the normal metal electron temperature, by measuring the power reflected from the circuit at the  $LC$  resonance frequency. A change of the junction resistance  $R_0$ , induced by heating the electrons, in turn changes the amplitude of the reflected radio frequency signal. In this technique, the stray cable capacitance  $C$  is in resonance with the inductor  $L$ , the resonator also serving to impedance-match the resistance of the tunnel junction to the measurement system. This readout scheme is analogous to that employed in the radio-frequency

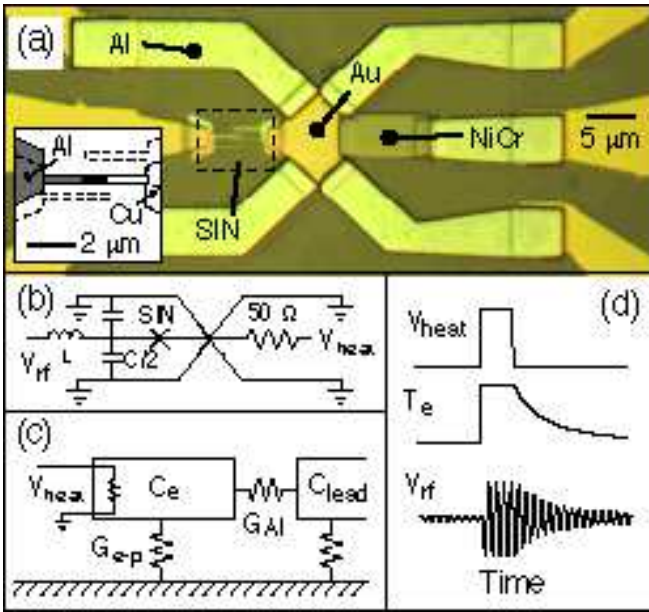


FIG. 1: (Color Online) (a) Optical micrograph of the electron calorimeter. The center Au island is contacted on the left by a rf-SIN thermometer, and on the right by a NiCr resistor. The outer ground leads and the contact right of the resistor are superconducting Al. *inset*: Detail drawing of the SIN junction, Al shown in gray, Cu in white, and overlap junction area in black. The dotted outlines are fabrication artifacts. (b) Electrical circuit. The SIN thermometer is embedded in an  $LC$  resonator formed by a discrete inductor and the stray lead capacitance. The junction resistance is monitored using the power reflected from the  $LC$  resonator at its resonance frequency. (c) Thermal schematic. The calorimeter electron gas  $C_e$  is thermally isolated by the superconducting Al contacts ( $G_{Al}$ ); the dominant thermal link is thus through the substrate phonons ( $G_{e-p}$ ). The NiCr resistor directly heats the electron gas. (d) Timing diagram. The voltage pulse applied to the heater causes the temperature to rise, saturate, and then decay. The envelope of the reflected power from the  $LC$  resonator is directly related to the temperature.

single electron transistor (rf-SET) [13].

Our device is fabricated on a  $4 \times 4 \times 0.5 \text{ mm}^3$  single-crystal GaAs chip using four lithography steps. A 85 nm thick Au center island and wire-bond pads were first deposited on the GaAs substrate; an intermediate Au pad was also deposited in this layer. We then deposited a 100 nm thick NiCr film, designed to have a  $50 \Omega$  resistance, matching the characteristic cable impedance  $Z_0$ . The ground leads and heater contact were evaporated in the third layer, using superconducting Al to ensure thermal isolation below 1 K [14]. The NiCr contacts the Al *via* the intermediate Au pad, to ensure low interfacial resistivity. The tunnel junction thermometer was deposited in the fourth lithography step. We used a standard suspended resist bridge, double-angle evaporation method to define the tunnel junction [15]: A 90 nm thick Al electrode was evaporated, and the Al then oxidized in 200 mTorr of pure  $\text{O}_2$  for 90 s. The junction was completed by evaporating a 90 nm thick Cu counterelectrode, which also contacted the center Au island.

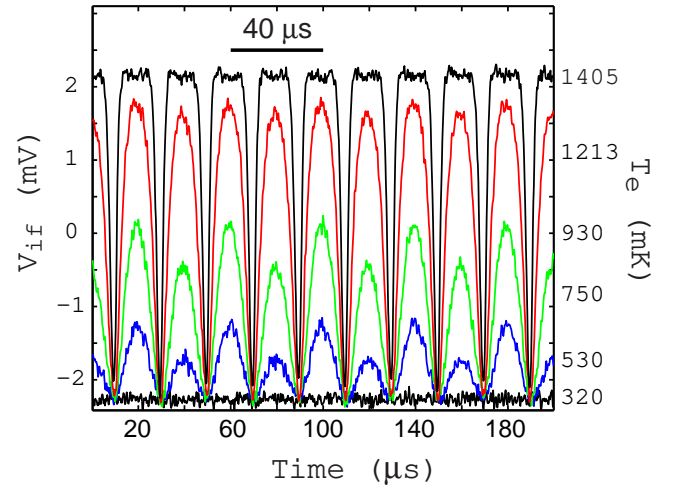


FIG. 2: (Color Online) Response to a 25 kHz heater drive (*left axis*: Mixer if voltage, *right axis*: Electronic temperature). The thermometer response is at 50 kHz as discussed in the text. Each trace is the result of 256 averages with a 2 MHz low-pass filter. The baseline signal is for zero heater power, with power ranging from 300 pW to 100 nW. At the highest power the signal clips at  $T = T_C \approx 1400$  mK. The 25 kHz components at low power are due to a dc offset in the heater signal.

The device is shown in Fig. 1(a). Note that the Au center island is electrically grounded, so that heating signals applied to the NiCr resistor do not couple directly to the SIN junction, but instead affect it by changing the temperature of the Au island. The heating signals are in principle therefore limited by diffusion time from the NiCr through the Au island and then along the Cu electrode to the SIN tunnel junction; we estimate this time to be less than 10 ns.

We mounted the chip containing the device on a printed circuit board, which was enclosed in a brass box. Gold wire bonds ( $25 \mu\text{m}$  diameter) were made between the Au bond pads on the chip and Cu coplanar striplines on the circuit board. A chip inductor with  $L = 390$  nH was placed in series with the SIN junction. The resonance capacitance  $C$  was from the geometric capacitance of the stripline and Au bond pads, with  $C = 0.5$  pF. The expected  $LC$  resonance frequency is  $f_{res} = 1/2\pi(LC)^{1/2} \approx 350$  MHz, the tuned circuit quality factor is  $Q = \sqrt{L/CZ_0^2} \approx 20$ , and the measurement bandwidth is  $\Delta f = f_{res}/Q \approx 20$  MHz. The measurement circuit is shown in Fig. 1(b). The tunnel junction is configured for simultaneous dc and rf measurements *via* a bias tee, not shown in Fig. 1.

We have described the technical aspects of rf-SIN thermometry elsewhere [5]. Here we will describe the salient aspects as they pertain to these measurements. We determined the resonance frequency of the  $LC$  circuit to be 345 MHz. A carrier signal source was connected through a directional coupler to a coaxial line, which was in turn connected to the  $LC$  resonant circuit. The carrier frequency was set close to the  $LC$  resonant frequency [16]. The signal reflected from the  $LC$  resonator was high-pass filtered and amplified using

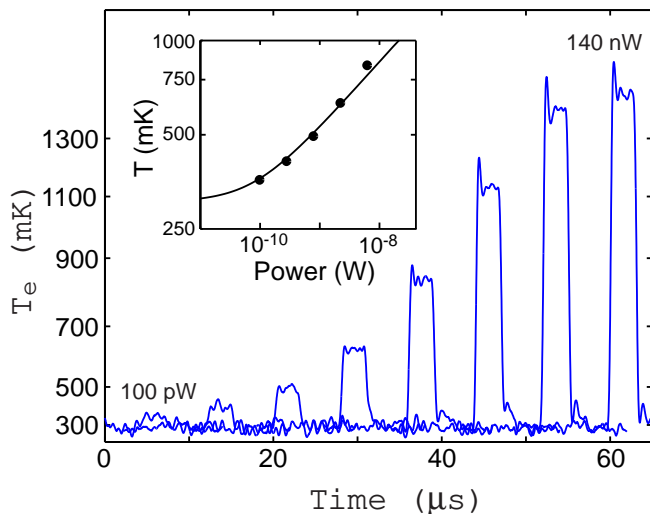


FIG. 3: Composite response to pulsed heating signals, with pulses  $3.0 \mu\text{s}$  long with peak power 0.1, 0.3, 0.8, 2.2, 6.2, 17.6, 49.0, and 140 nW. The resulting electronic temperature for each pulse is used to determine the relation  $P(T_e, T_p)$ . *Inset*: The solid line is a fit to  $P(T_e, T_p) = V\Sigma(T_e^n - T_p^n)$ , with  $T_p = 300 \text{ mK}$ ,  $n = 4.7$ ,  $V = 10 \mu\text{m}^3$ , and  $\Sigma = 2.1 \times 10^9 \text{ W/m}^3\text{-K}^{4.7}$ .

a low-noise amplifier. This amplified signal was then mixed with a local oscillator (lo), provided by a second rf signal source phase-locked to the carrier source. The intermediate frequency (if) output from the mixer was low-pass filtered, amplified, and the resulting time-dependent signal captured by a sampling oscilloscope. The NiCr resistor was heated using either a dc or an rf pulsed source: A pulse sent to the resistor heats the NiCr, the Au island and the Cu electrode, changing the electron temperature, and therefore changing the amplitude of the carrier signal reflected from the tuned  $LC$  circuit, as shown in Fig. 1(d).

In order to characterize the response of the system, we first heated the NiCr resistor using a  $f_0 = 25 \text{ kHz}$  sinusoidal drive signal. Figure 2 shows the response for various drive powers. The if signal was low-pass filtered ( $f < 2 \text{ MHz}$ ), and each curve is the result of averaging 256 drive periods. The left axis is the mixer if voltage, and the labels on the right axis indicate the electron temperature inferred from the change in reflected signal. The instantaneous power dissipated in the resistor is proportional to the square of the voltage applied the heater ( $P(t) = V^2(t)/R_{\text{NiCr}}$ ); this causes the reflected signal to be modulated at twice the heater signal,  $2f_0 = 50 \text{ kHz}$ . At low powers  $P$ , contributions at  $25 \text{ kHz}$  were also present, due to a small dc offset on the heater voltage  $V(t)$ ,  $V(t) = V_{\text{dc}} + V_0 \sin 2\pi f_0 t$ . At the highest powers, the reflected signal is clipped near the Al superconducting transition temperature: The junction resistance is temperature-independent above  $T_C$ .

The measured signal depends on the proper adjustment of the detection mixer's local oscillator (lo) phase. In order to correctly adjust this phase, we first applied a heater signal sufficient to get a clipped response. The phase of the lo was then adjusted to achieve maximum differential response be-

tween the lowest ( $\cong 300 \text{ mK}$ ) and highest ( $\cong 1400 \text{ mK}$ ) electron temperatures. The SIN junction ranges from  $105 \text{ k}\Omega$  to  $6 \text{ k}\Omega$  over this temperature range, and passes through the value of  $R_0$  where optimal matching with the cable impedance occurs [17]. In the parlance of radio-frequency electronics, the carrier signal is over-modulated, so the absolute value of the reflected power is a non-monotonic function of temperature. However, as we are sensitive to the phase of the carrier, the proper quadrature of the mixer if voltage does have a monotonic response. Finally, the reflected if signal as a function of cryostat temperature, for no heater voltage applied, was used to construct the temperature calibration,  $V_{if}(T)$ .

We measured the *quasi-static* relation between the electron-phonon power flow  $P_{e-p}$  and the electron and phonon temperatures,  $T_e$  and  $T_p$ , as given by Eq. (1). We applied a series of  $3 \mu\text{s}$  pulses while varying the peak heating power, and monitored the resulting time-dependent electron temperature. The substrate temperature was kept at  $300 \text{ mK}$ . The signal was filtered with a  $2 \text{ MHz}$  low-pass filter, and the result of 256 averages is shown in Fig. 2. This is equivalent to a dc heating measurement with a key difference, namely that as the heating pulses were delivered to the device at a  $1 \text{ kHz}$  repetition rate, the duty cycle was only  $0.3\%$ , so that the substrate phonons did not have sufficient time to heat. The equivalent measurement in a dc heating experiment requires 300 times as much power, with significant phonon heating a likely outcome. We find a fit relation matching that of Eq. (1), with  $n = 4.7$  and  $\Sigma = 2.1 \times 10^9 \text{ W/m}^3\text{-K}^{4.7}$ , in good agreement with previously measured values [3, 8, 9].

We finally performed measurements of *dynamic* electron-phonon cooling, by monitoring the detailed time-dependent behavior of the electron temperature at the end of a heating pulse. Figure 3 shows the measured response to a heater pulse (2560 averages, using a  $50 \text{ MHz}$  low-pass filter). The heating voltage pulse was configured to have  $1.6 \text{ ns}$  leading and trailing edge widths. The initial temperature rise is at least as fast as the time resolution of the measurement, with an expected rate  $\dot{T} = P/C_e \cong 140 \text{ mK/nsec}$ , as we are directly heating the electron population. The rapid onset also indicates that electron diffusion in the composite metal structure is not a rate-limiting factor. At the end of the pulse, the heating power drops to zero, leaving a non-equilibrium hot electron population that relaxes by phonon emission. Initially this relaxation is seen to be quite rapid, but it slows markedly as the electron temperature nears the phonon temperature.

The shape of the relaxation curve shown in Fig. 4 can be understood by examining the dynamics of the electron temperature. The electron heat capacity is  $C_e = \gamma VT_e$ , where  $\gamma$  is the Sommerfeld constant. The power flow to the phonons is given by Eq. (1). The time rate of change of the electron temperature  $\dot{T}_e$  is then

$$\dot{T}_e = -\frac{\Sigma}{\gamma} \left( T_e^{n-1} - \frac{T_p^n}{T_e} \right). \quad (2)$$

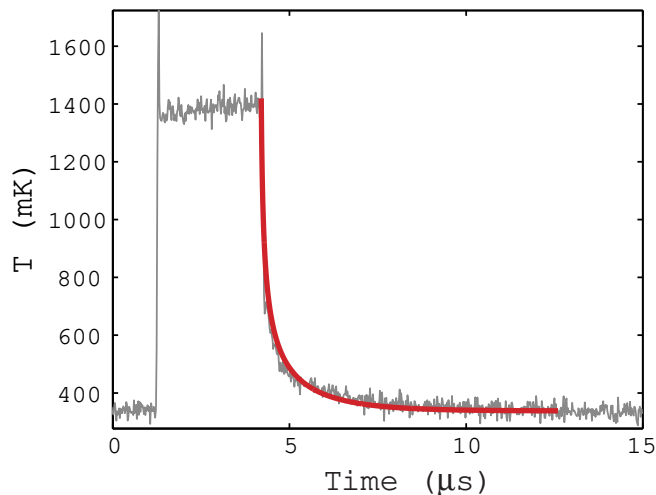


FIG. 4: (Color Online) Response to a  $3.0 \mu\text{s}$  pulse with peak power  $140 \text{ nW}$  applied to the heater. The electronic temperature quickly rises to  $\approx 1400 \text{ mK}$  at the start of the pulse. The trailing edge of the response decays with a temperature-dependent relaxation time. The solid line is a fit to the thermal model discussed in the text. The ringing is due to the if amplifier circuit.

Using the normalized temperature  $\theta \equiv T_e/T_p$ , this is

$$\dot{\theta} = -\frac{1}{n} \frac{1}{\tau_{e-p}(T_p)} (\theta^{n-1} - 1/\theta), \quad (3)$$

in terms of the small signal thermal relaxation rate  $\tau_{e-p}^{-1} = n\Sigma T_p^{n-2}/\gamma$  for electrons near the phonon temperature [18]. We fit our measured response to Eq. (3) using this rate as the only adjustable parameter, finding the value  $\tau_{e-p} = 1.6 \mu\text{s}$  [19]. This is in agreement with the measured value of  $\Sigma$ , and a composite  $\gamma$  which takes into account the relative metal volumes in the device. We can thus determine the the heat capacity of the metal island,  $C_e \sim 1 \text{ fJ/K} \cong 10^7 k_B$  at  $300 \text{ mK}$ .

There are some extremely interesting opportunities for electronic calorimetry in this temperature and size regime. Intriguing theoretical results have been presented for the thermodynamic response of mesoscopic superconducting disks [20], and giant moment electronic paramagnets such as PdMn [21] and PdFe [22] offer a means of probing the thermodynamics of a mesoscopic phonon-electron-spin-coupled system.

We are far from the ultimate calorimetric limits for this technique. Devices with active metal volumes that are smaller by a factor of  $10^4 - 10^5$  can be fabricated, yielding a total heat capacity of order  $\sim 10 - 100 k_B$  at  $30 \text{ mK}$ . Changes in the heat capacity of less than 10% are easily detected, yielding a sensitivity of order  $1 k_B$ , i.e. that associated with a single degree of freedom.

In summary, we have performed sub- $\mu\text{s}$  timescale measurements of the electron temperature of a micron scale metal island, cooled dynamically by phonon emission. The ability to apply and measure the response to fast heat pulses has permit-

ted us to directly measure the electron-phonon thermal relaxation, and thus extract the heat capacity of the metal island. This, to our knowledge, is the smallest measured heat capacity to date. The device that we have fabricated is a major step forward for mesoscopic thermodynamics, provides a platform for sub-aJ/K calorimetry, and can potentially play an important role in future single photon and phonon bolometers.

We acknowledge financial support provided by the NASA Office of Space Science under grants NAG5-8669 and NAG5-11426, the Army Research Office under Award DAAD-19-99-1-0226, and the Center for Nanoscience Innovation for Defense. We thank Bob Hill for processing support.

\* cleland@physics.ucsb.edu

- [1] L. G. C. Rego and G. Kirczenow, Phys. Rev. Lett. **81**, 232 (1998).
- [2] K. Schwab, E. A. Henriksen, J. M. Worlock, and M. L. Roukes, Nature **404**, 974 (2000).
- [3] C. S. Yung, D. R. Schmidt, and A. N. Cleland, Appl. Phys. Lett. **81**, 31 (2002).
- [4] A. N. Cleland, D. R. Schmidt, and C. S. Yung, Phys. Rev. B **64**, 172301 (2001).
- [5] D. R. Schmidt and C. S. Yung and A. N. Cleland, submitted to Appl. Phys. Lett.
- [6] W. A. Little, Can. J. Phys. **37**, 334 (1959).
- [7] V. F. Gantmakher, Rep. Prog. Phys. **37**, 317 (1974).
- [8] M. L. Roukes, M. R. Freeman, R. S. Germain, R. C. Richardson, and M. B. Ketchen, Phys. Rev. Lett. **55**, 422 (1985).
- [9] F. C. Wellstood, C. Urbina, and J. Clarke, Phys. Rev. B **49**, 5942 (1994).
- [10] M. Nahum and J. M. Martinis, Appl. Phys. Lett. **63**, 3075 (1993).
- [11] H. Pothier, S. Guéron, N. O. Birge, D. Esteve, and M. H. Devoret, Phys. Rev. Lett. **79**, 3490 (1997).
- [12] The intrinsic electrical bandwidth of a tunnel junction is set by the product of the tunnel resistance  $R_0$  and the junction capacitance  $C_J$ ,  $f_{3 \text{ dB}} = 1/2\pi R_0 C_J$ . For a fixed tunnel barrier thickness, this product is independent of the junction area  $A$ . With typical values of  $R_0 A \sim 10^3 \Omega - \mu\text{m}^2$  and  $C_J/A \sim 10^{-13} \text{ F}/\mu\text{m}^2$ , this corresponds to  $f_{3 \text{ dB}} \sim 2 \text{ GHz}$ .
- [13] R. J. Schoelkopf, P. Wahlgren, A. A. Kozhevnikov, P. Delsing, and D. E. Prober, Science **280**, 1238 (1998).
- [14] The thermal conductivity of superconducting Al is exponentially suppressed below  $T_C$ .
- [15] T. A. Fulton and G. J. Dolan, Phys. Rev. Lett. **59**, 109 (1987).
- [16] Typically -100 dB (100 fW), the rf-SET of Ref [13] can tolerate much higher power than the rf-SIN.
- [17] The calculated value is at  $R_0 = L/CZ_0 \sim 11 \text{ k}\Omega$ .
- [18] To recover the small signal response for  $n = 5$ , rewrite Eq. (2) in terms of the reduced temperature  $\epsilon \equiv (T_e - T_p)/T_p = \theta - 1$  and retain terms  $O(\epsilon)$ ,  $\dot{\epsilon} = 5(\Sigma/\gamma)T_p^{n-2}\epsilon$ .
- [19] For simplicity, we used  $n = 5$  for the fit.
- [20] P. S. Deo, J. P. Pekola, and M. Manninen, Europhys. Lett. **50**, 649 (2000).
- [21] G. J. Nieuwenhuys, Adv. Phys. **24**, 515 (1975).
- [22] R. P. Peters, C. Buchal, M. Kubota, R. M. Mueller, and F. Poell, Rev. Rev. Lett. **53**, 1108 (1984).